Supplementary Figure 1 - Ellisen et al.

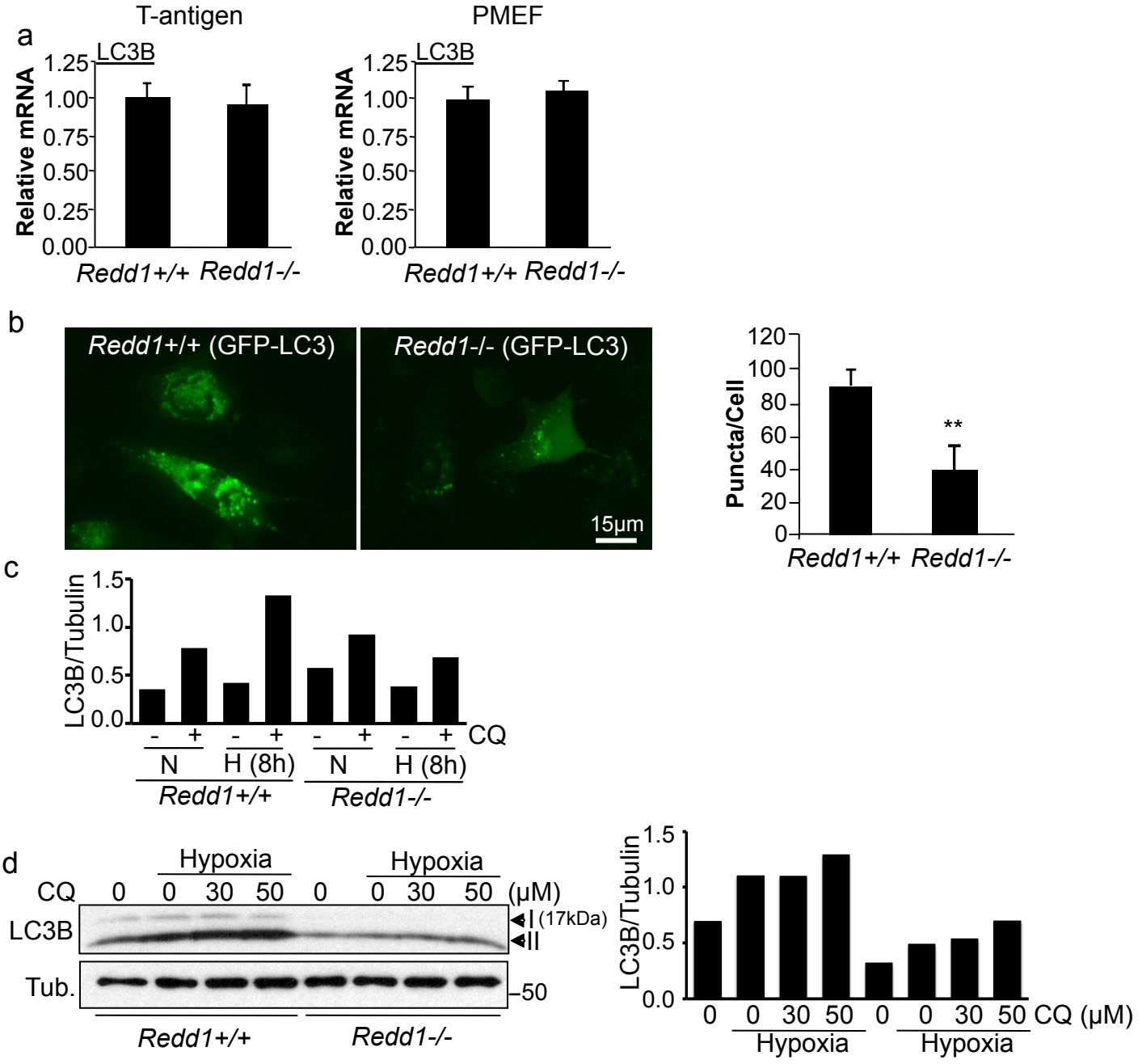

Supplementary Figure 1. Defective autophagy in *Redd1*$^{-/-}$ cells. (A). Reduced LC3B processing is not attributable to differences in LC3B mRNA expression between wild-type and *Redd1*$^{-/-}$ immortalized (left) and primary MEFs (right) as assessed by QRT-PCR. Error bars show SD of three measurements from experiments performed in duplicate. (B). Representative immunofluorescence images showing decreased GFP-tagged LC3 puncta in *Redd1*$^{-/-}$ cells as compared to wild-type cells cultured under basal conditions in the presence of CQ (30μM, 4h). N ≥ 20 cells counted per genotype. Scale bar, 15μm. (C). Densitometry analysis for Figure 1c. Bars show intensity of LC3B bands relative to β-Tubulin loading control. (D). Defective hypoxia-induced processing of LC3B in *Redd1*$^{-/-}$ cells. Cells were cultured hypoxia (1% O_2, 4h) and treated with the indicated concentrations of chloroquine (CQ, 4h). This experiment provides additional supportive data to Fig. 1c. Densitometry analysis is shown on the right panel. All error bars indicate SD. **P < 0.01 by paired t test (A, B)

Supplementary Figure 2 - Ellisen et al.

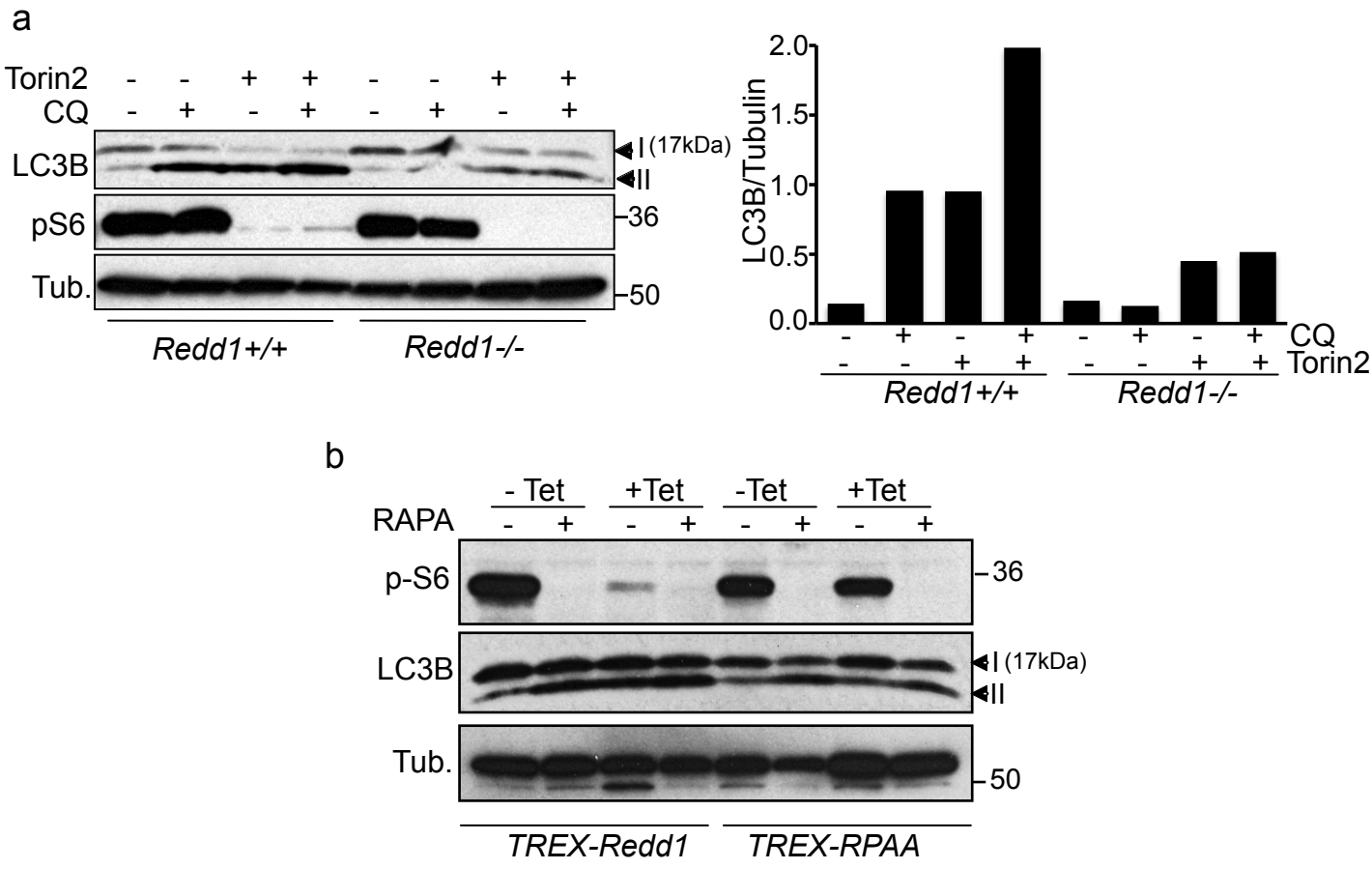

Supplementary Figure 2. REDD1 regulation of autophagy is largely mTORC1 independent. (A). Torin2 (25nM, 4h) does not rescue defective autophagic flux in *Redd1*$^{-/-}$ cells, as assessed by LC3B processing in the absence or presence of CQ (30μM, 4h). Activity of mTORC1 was assessed via phosphorylated ribosomal protein S6 (p-S6, S235/S236). β-Tubulin (Tub.) serves as a loading control. This experiment provides additional supportive data to Fig. 2b. Densitometry analysis of LC3B compared to loading control is shown at right. (B). Western blot analysis of endogenous p-S6 and LC3B corresponding to Figure 2d.

Supplementary Figure 3 - Ellisen et al.

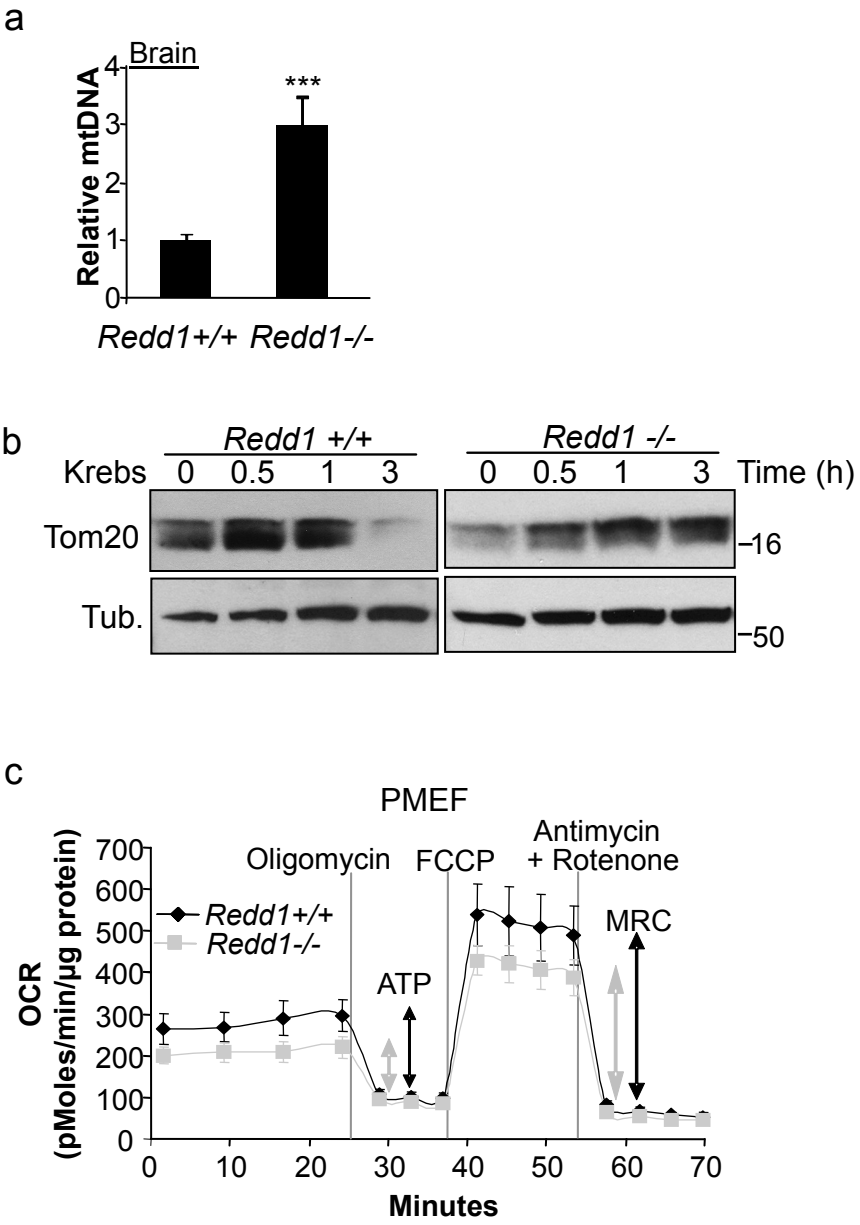

Supplementary Figure 3. Abnormalities in mitochondrial number and function in the absence of REDD1. (A). Increased mitochondrial number in brain of *Redd1*$^{-/-}$ mice, evidenced by increased mitochondrial to nuclear (M/N) DNA ratio (COXII/β-globlin) as measured by QRT-PCR. Error bars show SD of three measurements. (B). Failed mitochondrial clearance in *Redd1*$^{-/-}$ cells, evidenced by mitochondrial protein TOM20 levels upon starvation (Krebs solution) in wild-type and *Redd1*$^{-/-}$ MEFs. (C). Decreased basal and maximal O2 consumption rate in primary *Redd1*$^{-/-}$ MEFs. Respiration was assessed in the presence of mitochondrial inhibitors oligomycin (0.25µM), uncoupler FFCP (5µM), antimycin A (1µM) and rotenone (1µM). This experiment shows additional supportive data to Fig. 3f. Error bars show SD of three measurements. ***$P < 0.001$ by paired t test. (A, C)

Supplementary Figure 4 - Ellisen et al.

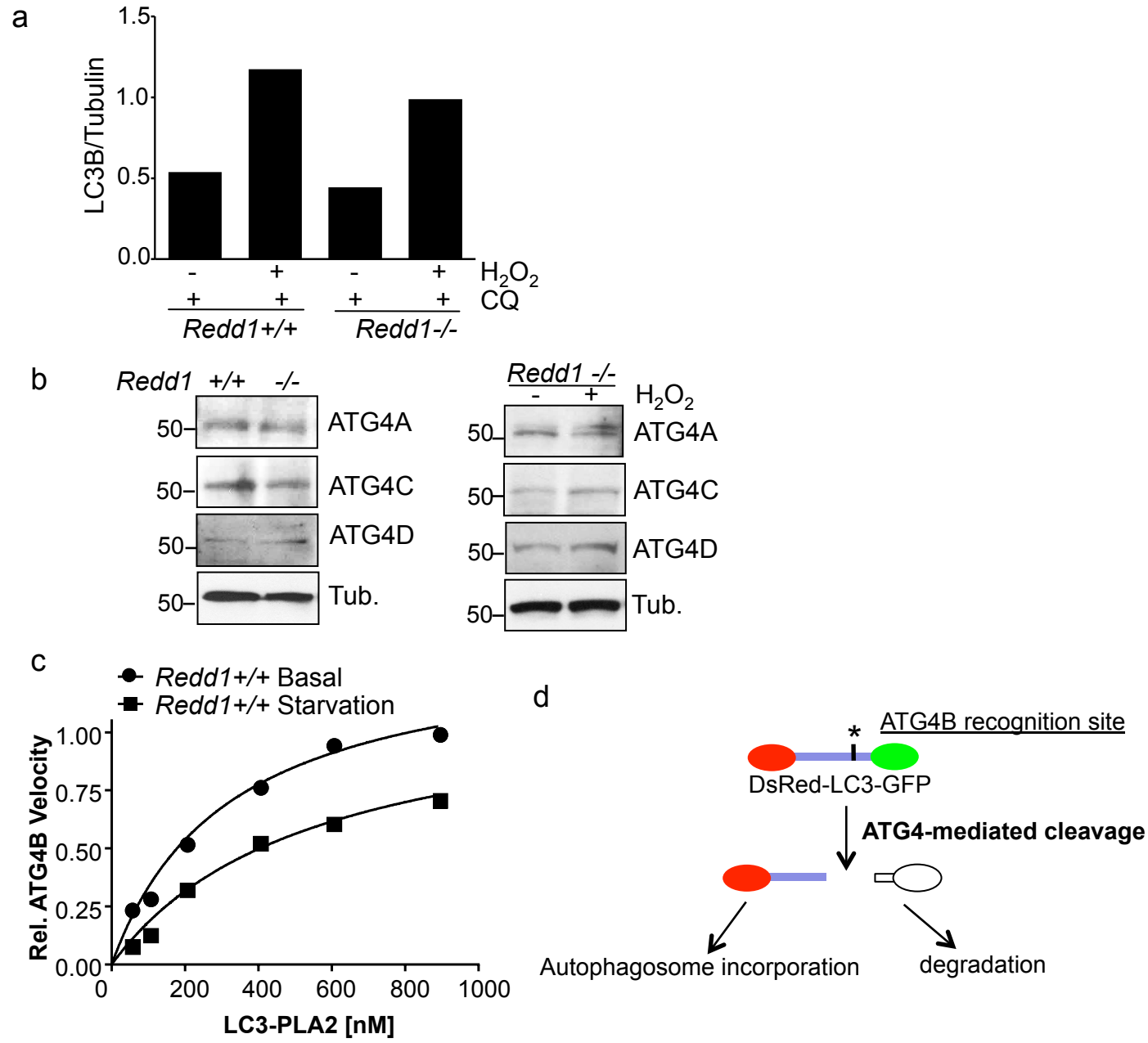

Supplementary Figure 4. ATG4 levels and suppression of ATG4B activity under starvation. (A) Densitometry quantitation for Figure 4f. (B) Western blot analysis showing similar levels of ATG4 family members in wild-type and *Redd1*$^{-/-}$ MEFs at basline and following H_2O_2 treatment (3mM, 6h). (C) ATG4B activity is suppressed in wild-type cells cultured under starvation (0.1%, FBS, 24h) as compared to cells cultured under basal condition (10% FBS). Cellular extracts were incubated with LC3-PLA_2 substrate at indicated concentrations and determination of kinetic parameters for Vmax by nonlinear regression of fitted curves as described in methods. (D) Schematic representation of LC3 processing assaying using double fluorescent tagged DsRed-LC3-GFP. ATG4B cleaves unprocessed LC3 to generate a DsRed-tagged N-terminal fragment and a C-terminal fragment subject to rapid degradation. Thus, the basal GFP/RFP ratio measured by flow cytometry in cells expressing this construct is inversely proportional to ATG4B enzymatic activity.

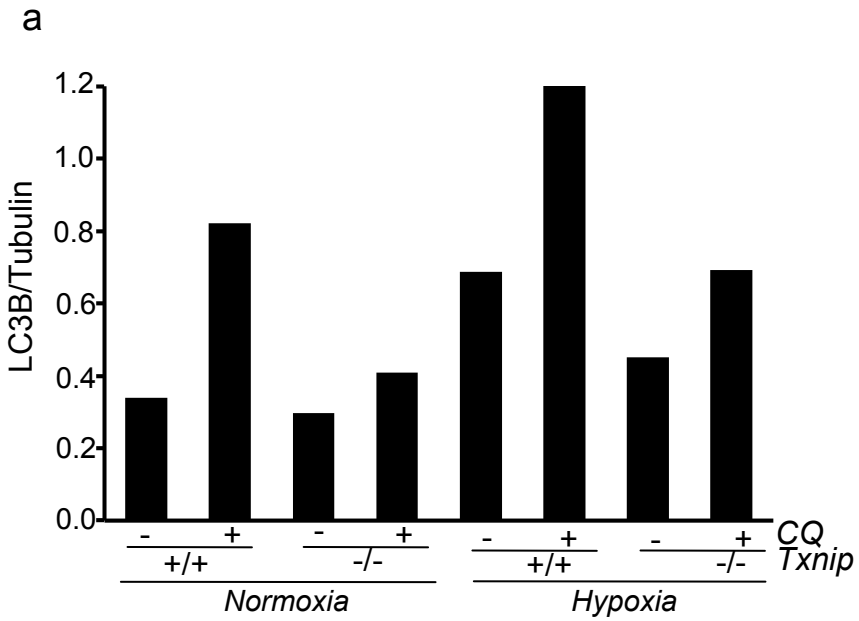

Supplementary Figure 5. Defective autophagy in *Txnip*$^{-/-}$ cells.
Densitometry quantitation of LC3B compared to loading control for Figure 5h.

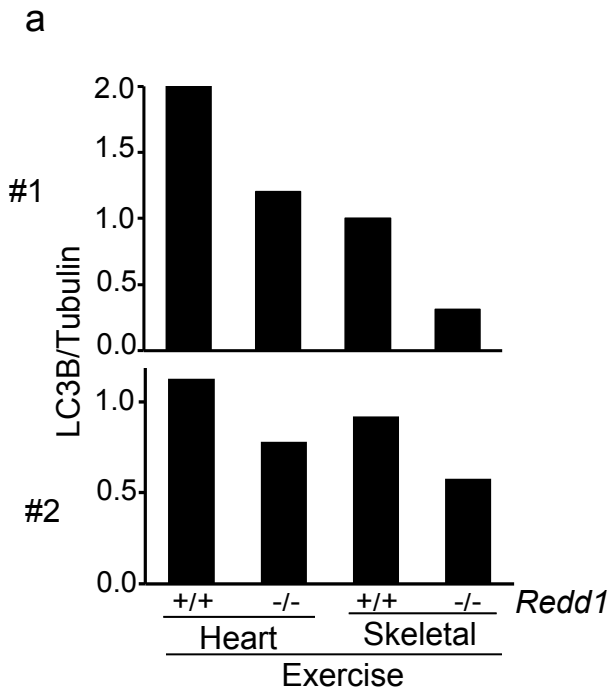

Supplementary Figure 6. Defective autophagy in *Redd1*$^{-/-}$ tissue.
Densitometry quantitation of LC3B compared to loading control for Figure 6f.

Supplementary Figure 7 - Uncropped blots

Fig 1a

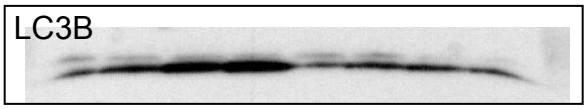

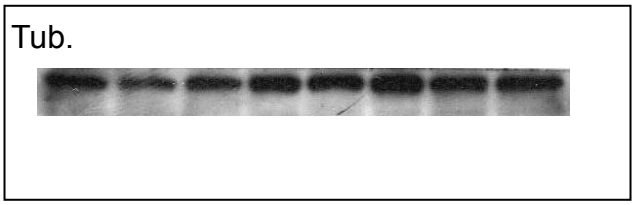

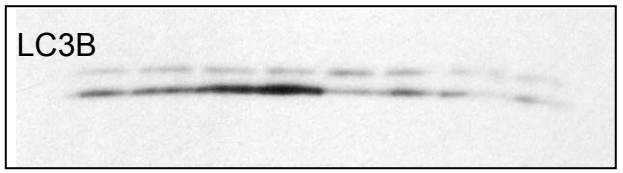

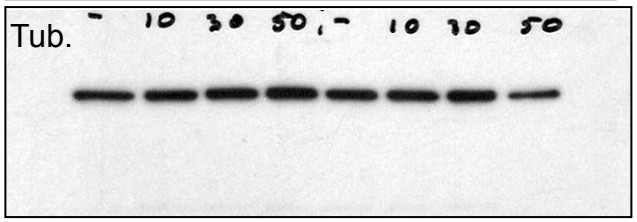

Fig 1c

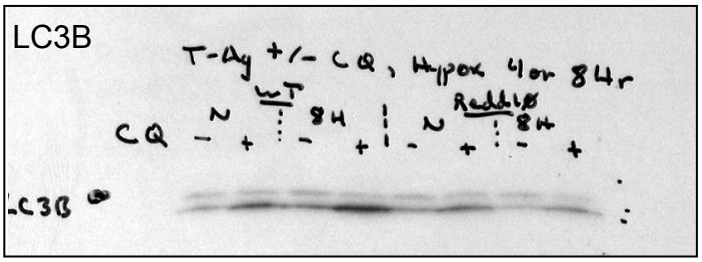

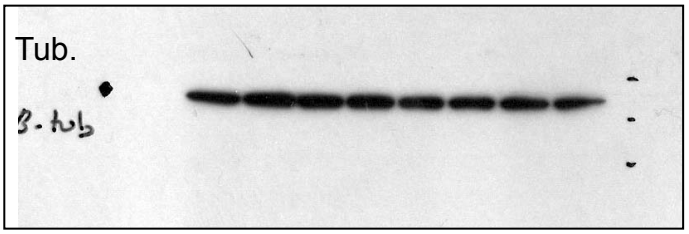

Fig 1e

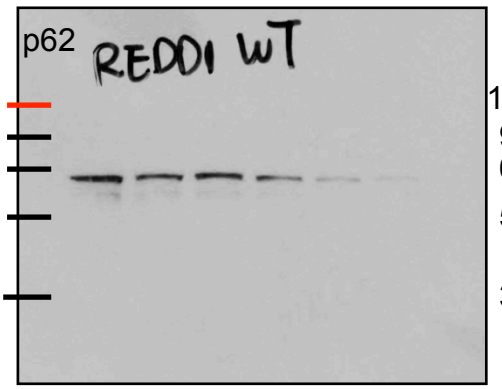

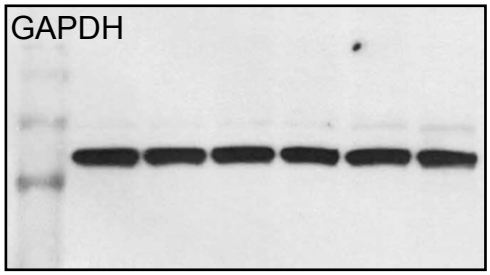

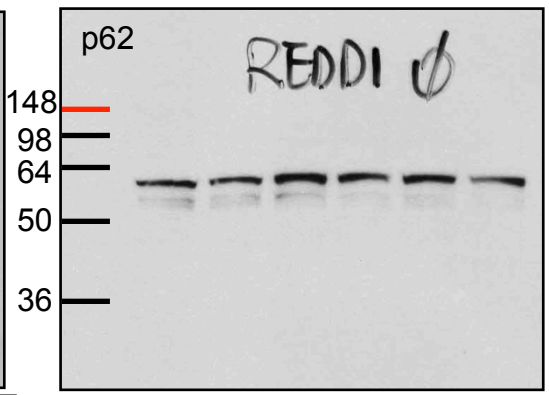

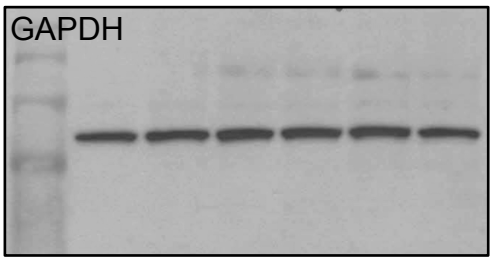

Fig 1f

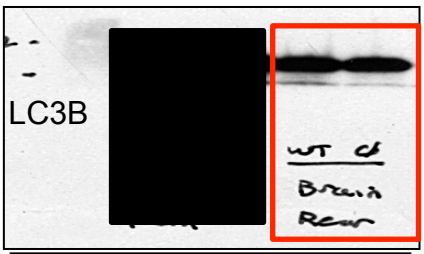

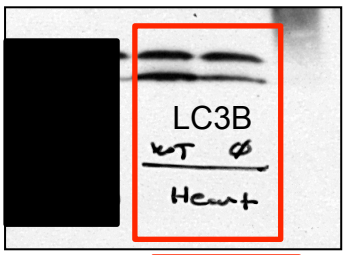

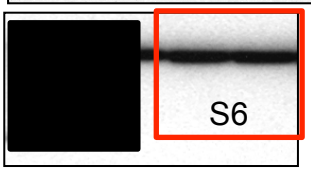

Supplementary Figure 7 - Uncropped blots

Fig 1f

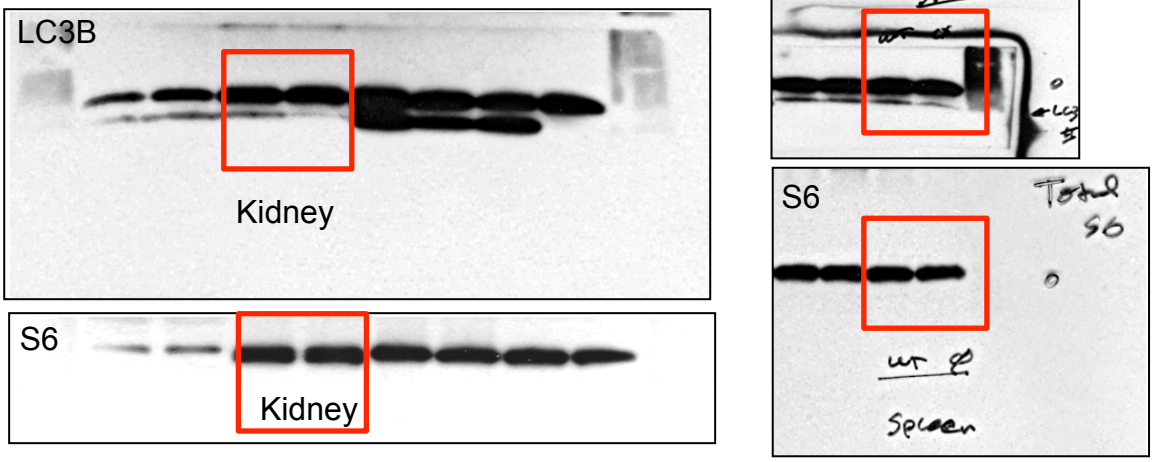

Fig 3a

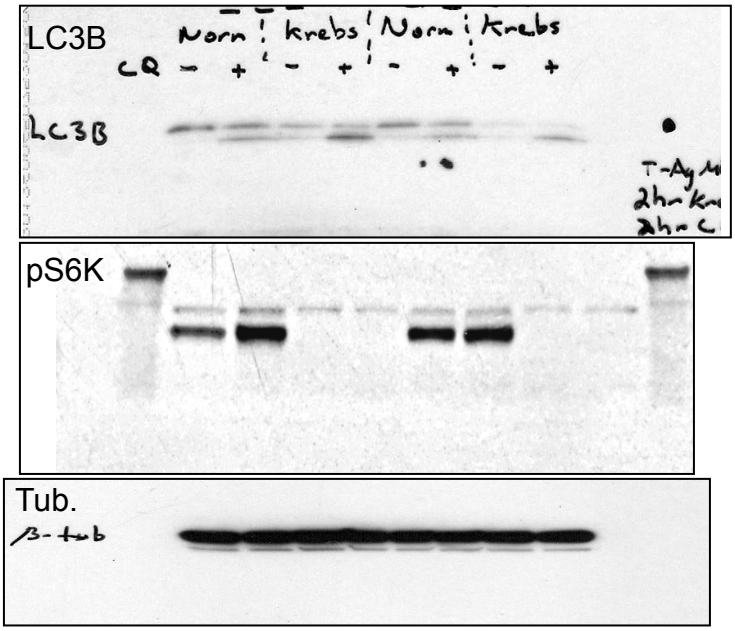

Fig 3b

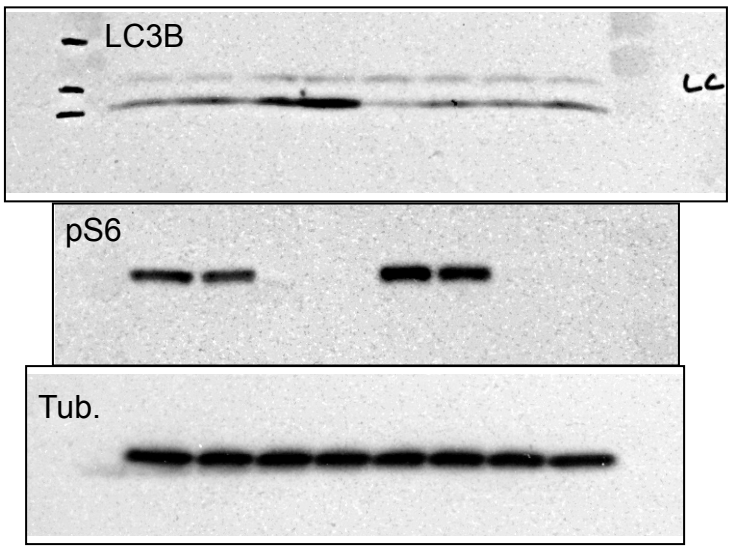

Supplementary Figure 7 - Uncropped blots

Fig 4f

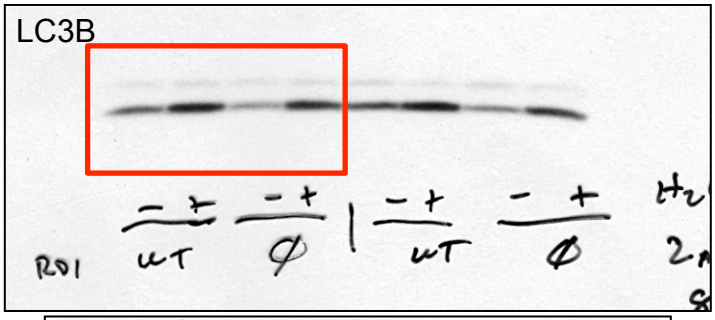

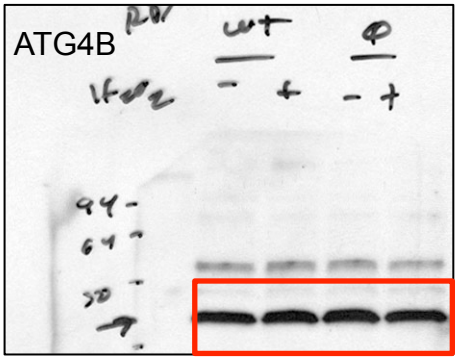

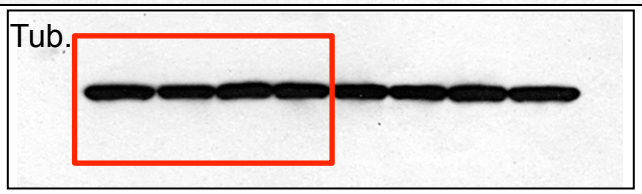

Fig 5h

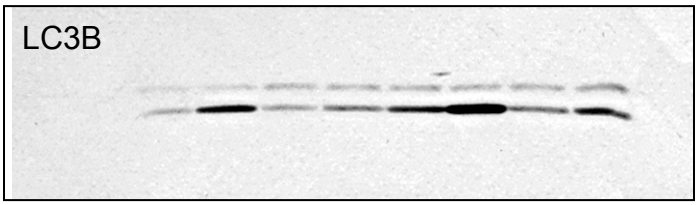

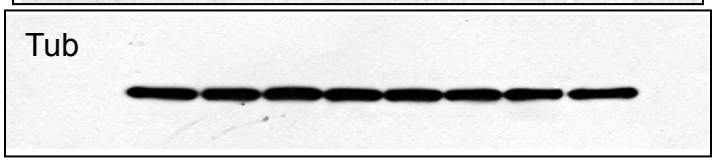

Fig 5j

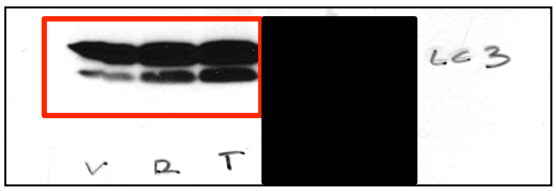

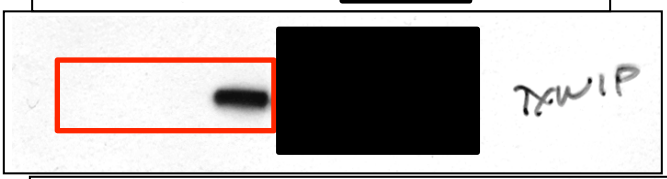

Supplementary Figure 7 - Uncropped blots

Fig 6a

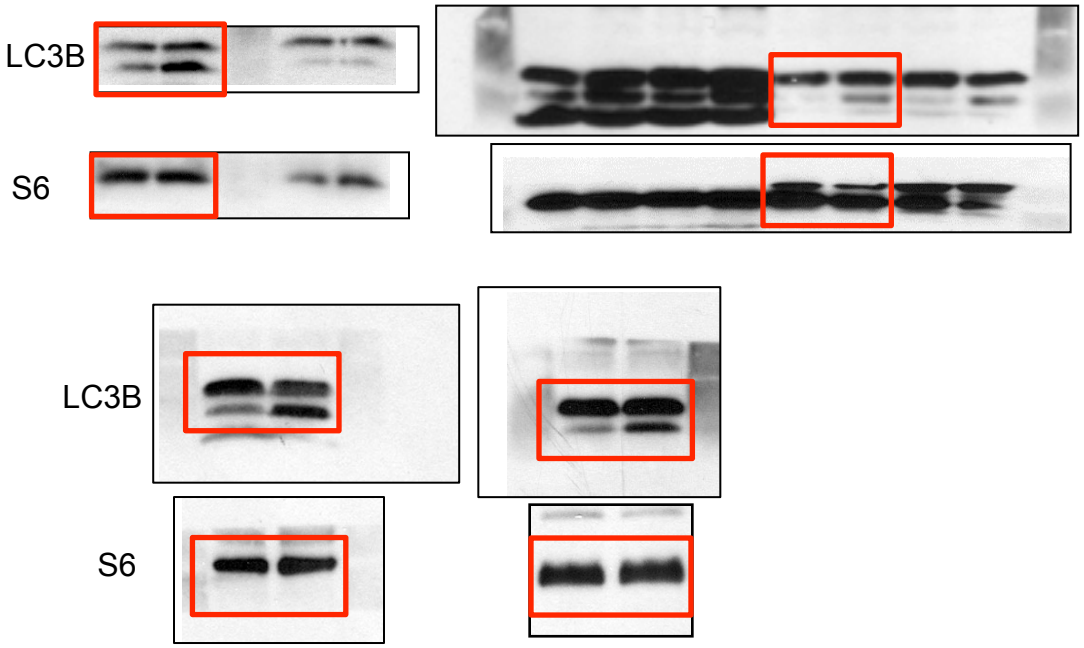

Fig 6f

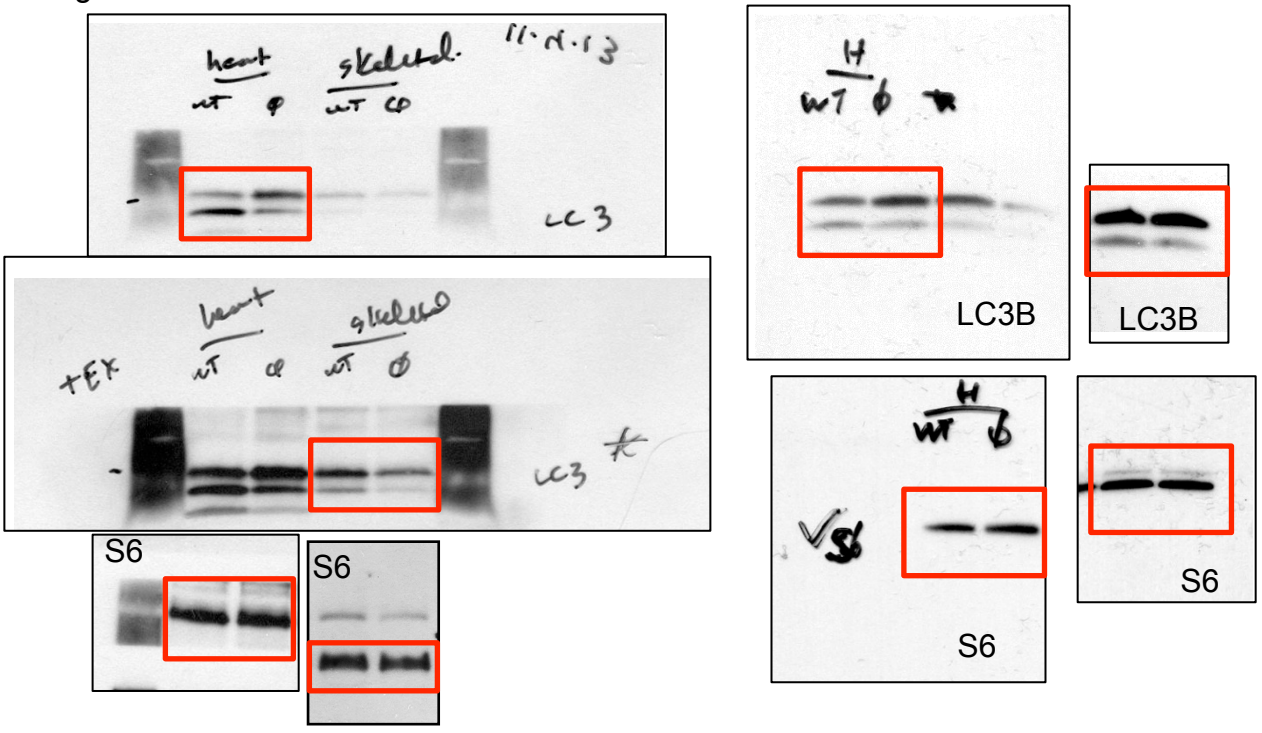

Supplementary Figure 7 - Uncropped blots

Fig S1d

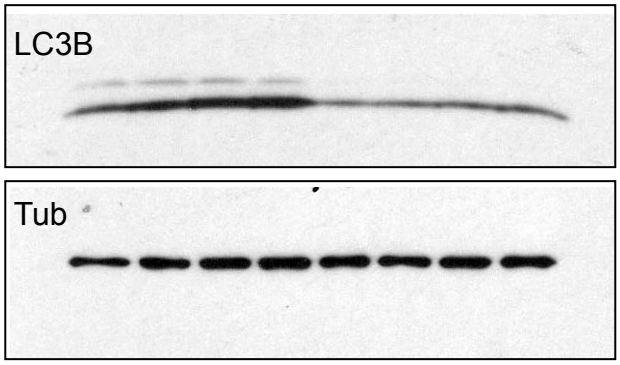

Fig S2a

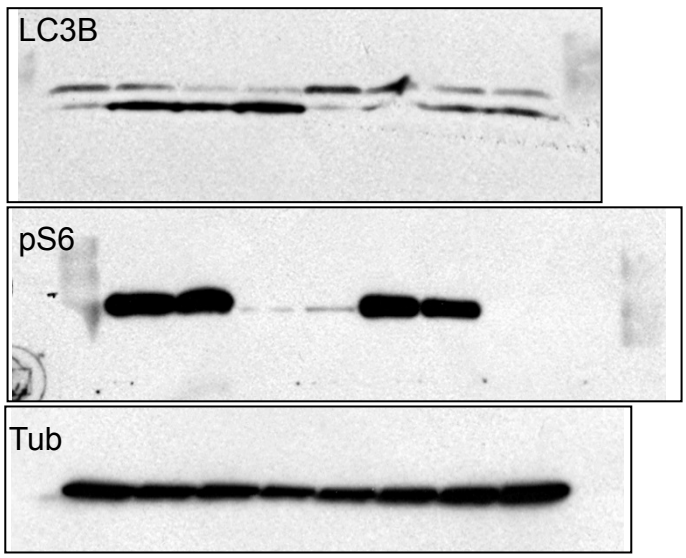

Fig S3b

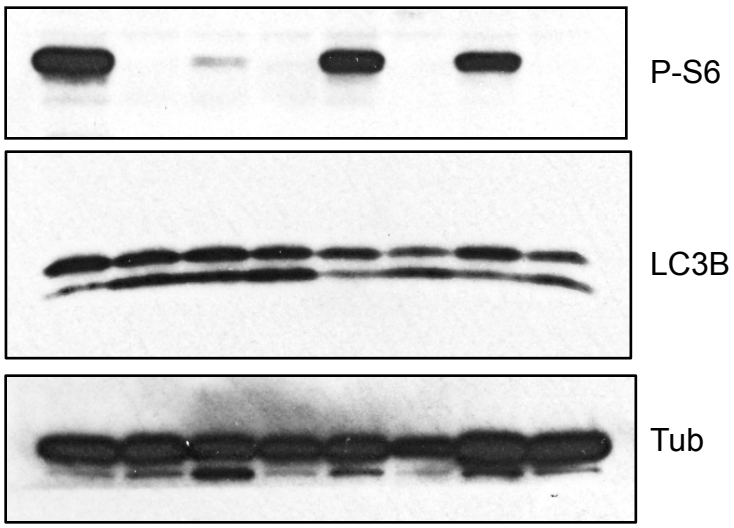

Supplementary Figure 7 - Uncropped blots

Fig S3b

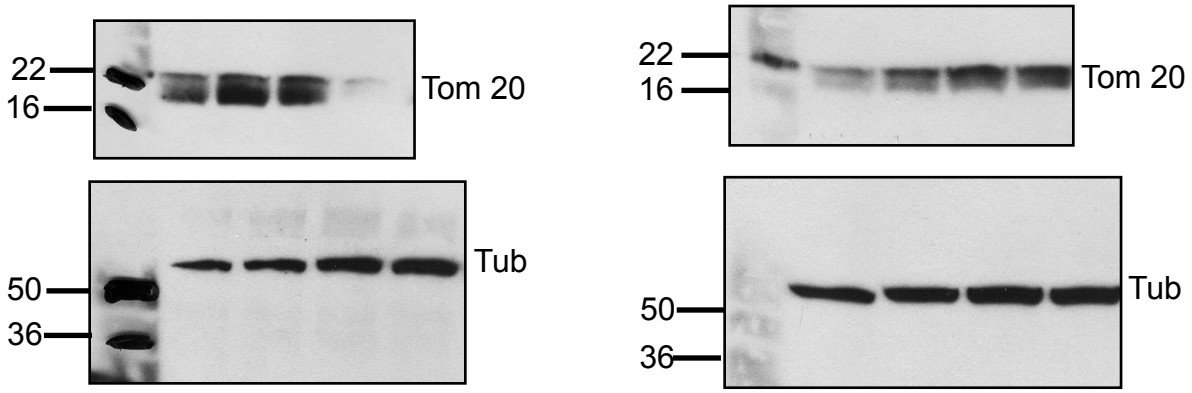

Fig S4b

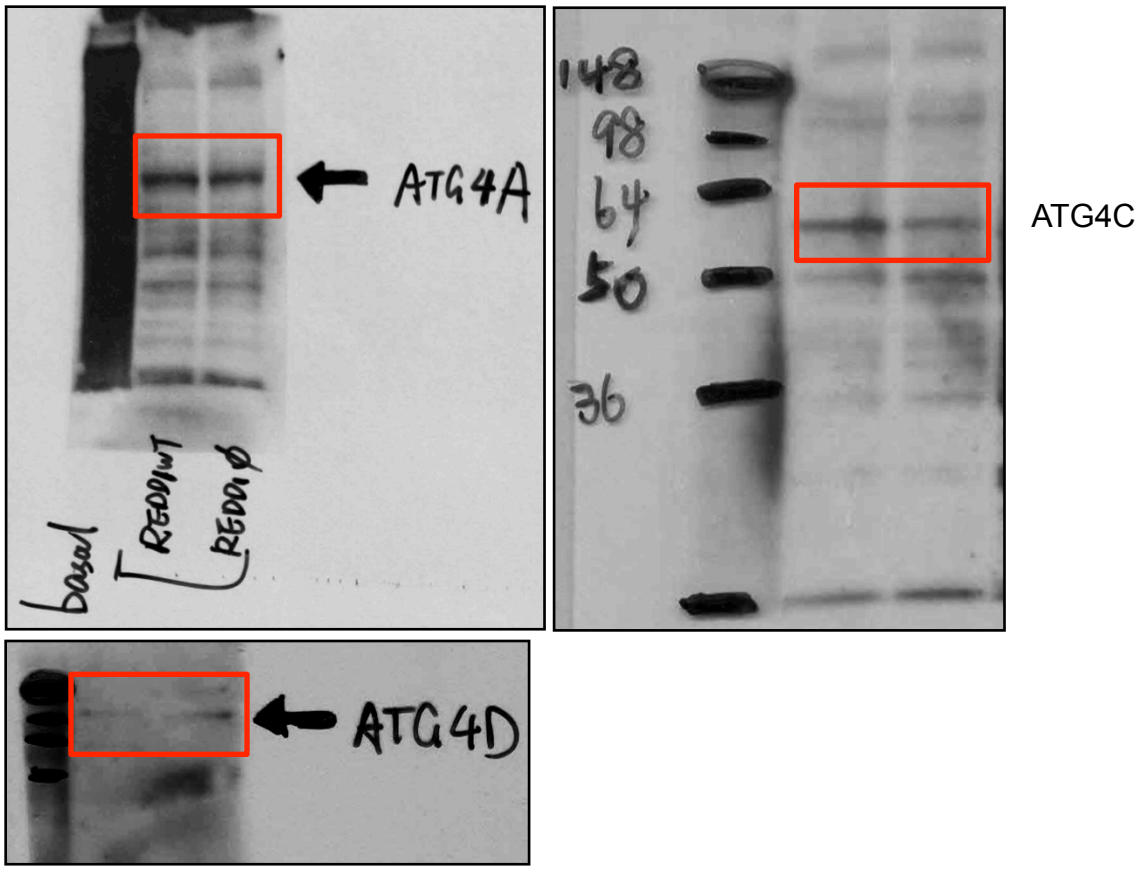

Supplementary Figure 7 - Uncropped blots

Fig S4b